Discovery of New Inhibitors of D-Alanine:D-Alanine Ligase by Structure-Based Virtual Screening†

Andreja Kovač,‡ Janez Konc,§ Blaž Vehar,§ Julieanne M. Bostock,|| Ian Chopra,|| Dušanka Janežič,§ and Stanislav Gobec*,‡

University of Ljubljana, Faculty of Pharmacy, Aškerčeva 7, 1000 Ljubljana, Slovenia, National Institute of Chemistry, Hajdrihova 19, 1000 Ljubljana, Slovenia, and Institute of Molecular and Cellular Biology and Antimicrobial Research Centre, University of Leeds, Leeds LS 9JT, U.K.

Received June 16, 2008

The terminal dipeptide, D-Ala-D-Ala, of the peptidoglycan precursor UDPMur*N*Ac-pentapeptide is a crucial building block involved in peptidoglycan cross-linking. It is synthesized in the bacterial cytoplasm by the enzyme D-alanine:D-alanine ligase (Ddl). Structure-based virtual screening of the NCI diversity set of almost 2000 compounds was performed with a DdlB isoform from *Escherichia coli* using the computational tool AutoDock 4.0. The 130 best-ranked compounds from this screen were tested in an in vitro assay for their inhibition of *E. coli* DdlB. Three compounds were identified that inhibit the enzyme with K_i values in micromolar range. Two of these also have promising antibacterial activities against Gram-positive and Gram-negative bacteria.

Introduction

The appearance of drug-resistant bacteria is a strong motive for the development of new antimicrobial agents. A well-validated target for antibacterial therapy is the system of enzymes responsible for the construction of peptidoglycan, an essential component of the bacterial cell wall that provides the structural integrity that is necessary for bacterial cells to resist internal osmotic pressure.[1] In contrast with the extracellular stages of peptidoglycan biosynthesis, which are inhibited by β-lactam and glycopeptide antibiotics, the early intracellular steps of peptidoglycan synthesis have received less attention as potential drug targets so far. Only two drugs that inhibit intracellular steps of peptidoglycan synthesis are currently used: fosfomycin, an inhibitor of MurA ligase, the enzyme that adds phosphoenolpyruvate on UDP-*N*-acetylglucosamine in the first step of its modification into the cell wall precursor UDP-*N*-acetylmuramic acid (UDP-Mur*N*Ac[a]), and D-cycloserine, which inhibits both alanine racemase and D-alanine:D-alanine ligase (Ddl). Mur ligases, including MurC, MurD, MurE, and MurF, assemble the final intracellular peptidoglycan precursor UDP-Mur*N*Ac-pentapeptide by the successive addition of L-Ala, D-Glu, *m*-Dpm or L-Lys and D-Ala-D-Ala to UDP-Mur*N*Ac. Ddl is responsible for supplying the MurF substrate, D-alanyl-D-alanine. This terminal dipeptide plays a crucial role in the assembly of the bacterial cell wall because cross-linking of peptidoglycan chains occurs between the C_6-ε-NH_2-group of *meso*-diaminopimelic acid (in Gram-negative bacteria) or the NH_2 group of pentaglycine (in Gram-positive *Staphylococcus*) and the penultimate D-Ala in a second pentapeptide strand. In both cases, the intrastrand D-Ala-D-Ala bond is broken, and a new interstrand peptide bond is formed (DAP-ε-NH-D-Ala or $(Gly)_5$-D-Ala).[2−5]

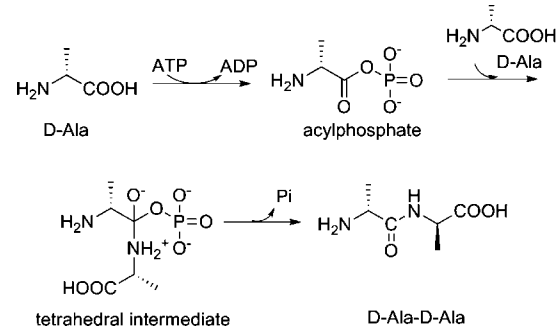

Figure 1. Mechanism of catalysis of DdlB.

In *Escherichia coli* and *Salmonella typhimurium*, two Ddl isoforms, DdlA and DdlB exist with similar kinetic characteristics and substrate specificity. The alignment of the predicted amino acid sequences of *E. coli* DdlA and DdlB reveals approximately 35% identity between both enzymes. Because both show similar susceptibility to known inhibitors and crystal structures of only the wild-type *E. coli* DdlB and its Y216F mutant derivate have been reported, we focused our attention on the DdlB isoform.[6,7]

The dimerization of D-alanine begins with an attack on the first D-alanine by the γ-phosphate of adenosine triphosphate (ATP) to give an acylphosphate (Figure 1). This is condensed with the second D-alanine amino group, eliminating the phosphate and yielding D-alanyl-D-alanine.[8,9] To avoid depletion of L-alanine, which is the biosynthetic precursor of D-alanine, the Ddl is strongly inhibited by its reaction product D-Ala-D-Ala.[10] Mutation of Ddl leads to the structurally related D-alanyl-D-lactate ligases (VanA, VanB, VanD) and D-alanyl-D-serine ligases (VanC, VanE, VanG). Replacement of the terminal D-Ala-D-Ala dipeptide with either the depsipeptide D-Ala-D-Lac

† Dedicated to Professor Slavko Pečar on the occasion of his 60th birthday.

* To whom correspondence should be addressed. Tel: +386 1 4769 585. Fax: +386 1 4258 031. E-mail: gobecs@ffa.uni-lj.si.

‡ University of Ljubljana.

§ National Institute of Chemistry.

|| Institute of Molecular and Cellular Biology and Antimicrobial Research Centre.

[a] Abbreviations: UDPMur*N*Ac, uridinediphosphate-*N*-acethylmuramic acid; MurA, UDP-*N*-acetylglucosamine enolpyruvyltransferase; Ddl, D-alanine:D-alanine ligase; MurC, UDP-*N*-acetylmuramate:L-alanine ligase; MurD, UDP-*N*-acetylmuramoyl-L-alanine:D-glutamate ligase; MurE, UDP-*N*-acetylmuramoyl-L-alanine-D-glutamate:2,6-diaminopimelate/L-Lys ligase; MurF, UDP-*N*-acetylmuramoyl-L-alanine-D-glutamyl-2,6-diaminopimelate/L-lysine:D-alanyl-D-alanine ligase; VanA, VanB, VanD, D-alanyl-D-lactate ligases; VanC, VanE, VanG, D-alanyl-D-serine ligases; NCI, National Cancer Institute; CROW, columns and rows of workstations; LGA, Lamarckian genetic algorithm; RA, residual activity.

10.1021/jm800726b CCC: $40.75
Published on Web 11/14/2008

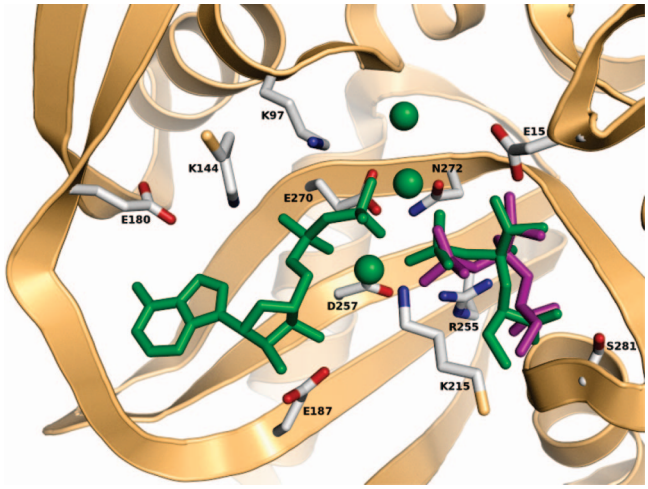

Figure 2. Control docking. The enzyme is shown with residues 141−157 and 207−217 omitted for clarity. ADP, POB, and the side chains of interacting residues are presented as sticks. Mg^{2+} ions are shown as spheres. The cocrystallized POB, ADP, and Mg^{2+} are green, and the docked POB in the lowest energy conformation is purple. Amino acid side chains are color coded by element: C, N, and O are gray, blue, and red, respectively.

or the dipeptide D-Ala-D-Ser leads to significantly reduced binding affinity for the glycopeptide antibiotic vancomycin and thus to vancomycin resistance.[11]

Few compounds that inhibit Ddl have been described. The most important inhibitor of Ddl is D-cycloserine (Scheme 1, **1**), a structural analogue of D-Ala.[12,13] Series of phosphinates (**2**), phosphonates (**3**), and phosphonamidates have been developed as transition-state analogue inhibitors or as analogues of D-alanyl phosphate.[14−17] It has been shown that transition-state mimetics can be phosphorylated by Ddl and inhibit the reaction by tightly binding the enzyme after the phosphorylation step.[18,19] Their antibacterial activities are low, but they allowed the crystallographic determination of complexes of *E. coli* DdlB with ADP/phosphorylated phosphinate and the *E. coli* Y216F DdlB mutant with ADP/phosphorylated phosphonate.[20,21] By the use of a de novo structure-based molecular design, a cyclopropane derivative (**4**) was developed as an inhibitor of DdlB, and an allosteric inhibitor of DdlB from *S. aureus* (**5**) was discovered by high-throughput screening and was cocrystallized with the enzyme.[22,23] Diazenedicarboxamides (**6**) were reported to be potent inhibitors of DdlB from *E. coli*, and they also possessed antibacterial activity.[24] Recently, protein kinase inhibitors (**7**) were also shown to be ATP-competitive inhibitors of DdlB.[25]

Faced with a growing need for new and more efficient antibacterial agents, we chose to take advantage of automated computational techniques to identify novel DdlB inhibitors as potential antibacterials. Structure-based virtual screening is primarily used as a hit-identification tool, but it can also be used for lead optimization and, when applied to structures such as cytochrome P450 isoforms, for the analysis of drug metabolism.[26,27] The aim of structure-based virtual screening is to reduce a large number of compounds to a smaller subset, which is more likely to contain biologically active compounds.

Virtual screening applied to the discovery of new enzyme inhibitors involves docking, computational fitting of structures of compounds to the active site of an enzyme, and scoring and ranking of each compound.[28] In this study, the AutoDock 4.0 docking program was employed in computation, and the NCI diversity set served as the compound library. The highest ranked compounds were tested for activity in a biochemical assay. Three structurally diverse compounds were discovered that inhibit DdlB with K_i values in the micromolar range. Two of the compounds were also shown to possess antibacterial activity against both Gram-positive and Gram-negative bacteria.

Materials and Methods

Computational Tools. Docking calculations were performed on 100 Intel Xeon processors, part of the CROW (columns and rows of workstations) Linux cluster at the National Institute of Chemistry, Ljubljana, Slovenia. Docking of 1990 compounds from the NCI diversity set took 2 days to complete with AutoDock 4.0. AutoDockTools package scripts were used to convert structures of compounds to AutoDock 4.0 format and to prepare proteins. AutoDock 4.0 was employed in the generation of grid files and in automated in silico docking and scoring (virtual screening). All figures were rendered using PyMOL.[29]

National Cancer Institute Diversity Set.[30] The National Cancer Institute (NCI) diversity set is a reduced library of 1990 compounds selected from the original NCI-3D structural database for their unique scaffolds. To date, the main use of the NCI Diversity Set has been in anticancer research.[31,32] The compounds are freely available as solutions in DMSO and are widely distributed to laboratories engaged in biomedical investigations as a research tool for various biological testing purposes related to cancer and opportunistic infections. Each compound in the NCI diversity set was docked to DdlB using AutoDock 4.0, and this resulted in a list of structures ranked according to their estimated free energies of binding.

Structures. We obtained structures of compounds from the NCI diversity set, which are available online in the AutoDock 3.0 format, and converted them to the AutoDock 4.0 format by using a script provided by the AutoDockTools package. From the diversity set prepared in this way, we deleted the compounds that were not promising candidates for further drug development (i.e., molecules containing arsenic, antimony, metals, etc.). We used the compounds' structures in the tautomeric state provided in the AutoDock-ready database of the NCI diversity set. This is a standard procedure employed in docking with AutoDock.[33,34]

Protein Preparation. The crystal structure of D-alanine:D-alanine ligase (DdlB) complexed with ADP/phosphorylated D-Ala-D-α-hydroxybutyrate phosphonate transition-state inhibitor resolved at 2.2 Å was retrieved from the Protein Data Bank (PDB code: 1iov). The inhibitor, the cofactor ADP, all water molecules, and the three Mg^{2+} ions cocrystallized at the binding site were removed, leaving only the residues of the DdlB enzyme. Preparation of the target protein with the AutoDockTools software involved the addition of polar hydrogen atoms to the macromolecule, a necessary step for the correct calculation of partial atomic charges. Gasteiger charges are calculated for each atom of the macromolecule in AutoDock 4.0 instead of Kollman charges, which were used in the previous versions of this program. Three-dimensional affinity grids of size 64 × 68 × 94 Å with 0.3 Å spacing were positioned around the active site and calculated for each of the following atom types: H, HD, C, A, N, NA, OA, F, P, SA, S, Cl, Br, and I, representing all possible atom types present in the NCI diversity set. AutoDock 4.0 distinguishes atoms that can accept hydrogen bonds (NA, OA, SA) and those unable to do so (N and S). It also distinguishes hydrogen atoms that can participate in a hydrogen bond (HD) and non-hydrogen-bonding hydrogen atoms (H). Additionally, an electrostatic map and a desolvation map were calculated.

Docking Protocol. AutoDock 4.0 was used for the docking simulation. We employed the Lamarckian genetic algorithm (LGA) for ligand conformational searching. LGA is a hybrid of a genetic algorithm and a local search algorithm. This algorithm first builds a population of individuals (genes), each gene being a different random conformation of the docked compound. The population undergoes simulated evolutionary development with processes of phenotypic mapping, fitness evaluation, natural selection, crossover, and elitist selection occurring in each generation. The local search

Scheme 1. Structures and Inhibitory and Antimicrobial Activities of Reported Inhibitors

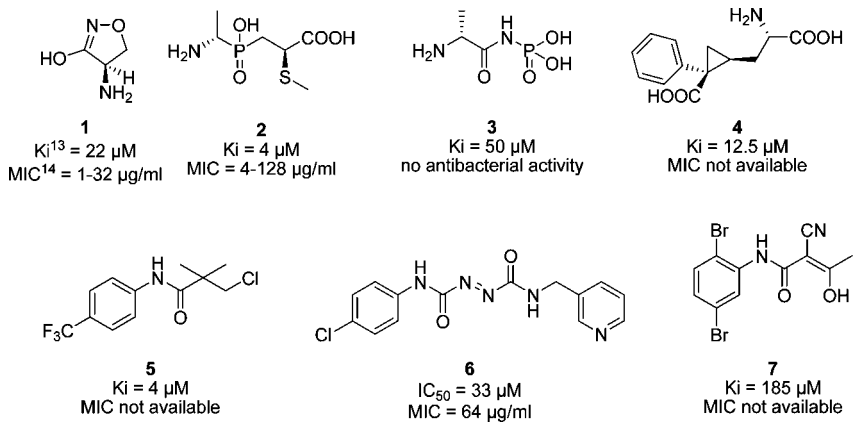

Table 1. Chemical Structures, Ranking of Hit Compounds, NSC Numbers, AutoDock Scores (Mean Estimated Free Energy of Binding), Calculated Physicochemical Properties (log P, PSA), K_i, and MIC Values

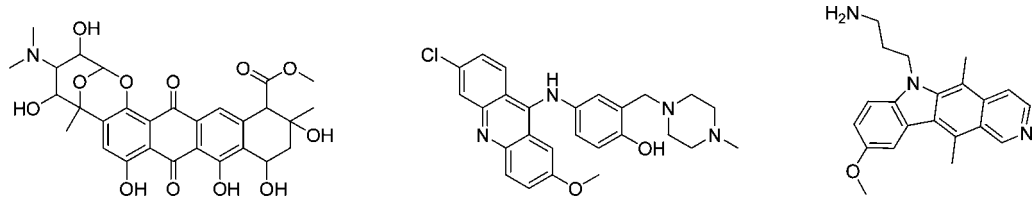

8 **9** **10**

compd	rank	NSC no.	AutoDock score (kcal/mol)	log P[a]	PSA (Å^2)[b]	K_i values for DdlB inhibition	MIC (μg/mL) *E. coli* 1411	MIC (μg/mL) *E. coli* SM 1411	MIC (μg/mL) *S. aureus* 8325-4
8	1	86 005	−18.34	0.6 ± 0.8	204	42 ± 5 μM (ATP competitive)	<256	<256	256
9	2	130 813	−16.02	4.7 ± 1.2	61	218 ± 14 μM (ATP noncompetitive)	<256	64	32
10	123	176 327	−8.87	3.7 ± 0.6	53	11 ± 1 μM (ATP competitive)	32	8	32

[a] log P was predicted using online property prediction tool ALOGPS 2.1.[50] [b] Online property prediction tool Molinspiration was used for calculation of PSA.[51]

algorithm then performs energy minimizations on a user-specified proportion of the population of individuals. Individuals with the lowest resulting energies are then transferred to the next generation, and the process is repeated. We set important docking parameters for the LGA as follows: population size of 150 individuals, maximum of 4 million energy evaluations, maximum of 27 000 generations, one top individual to survive to the next generation automatically, mutation rate of 0.02, crossover rate of 0.8, 100 docking runs, and random initial positions and conformations. The probability of performing a local search on an individual in the population was set to 0.06, and the maximum number of iterations per local search was set to 300. The docking jobs, one for each compound, were distributed to the CROW Linux cluster. Each docking job produced 100 docked conformations, which were clustered by the root-mean-square deviation (rmsd), which measured the difference between the coordinates of their constituent atoms, so that conformations in each cluster differed by less than 2.0 Å.

Materials. The 1990 compounds of the NCI diversity set were obtained as solutions in DMSO in 96-well microtiter plates from the National Cancer Institute. A plate contained 80 samples, each a 10 mM solution in 20 μL of 100% DMSO. Compounds that were detected as hits after the initial screening were acquired from the NCI as solid samples. The identities of five hit compounds that were identified after the initial screening were investigated by mass spectroscopy, ^{1}H NMR spectroscopy, or both. The ^{1}H NMR and mass spectra were found to be inconsistent with the reported structures for two of the five compounds. The structures of the confirmed three hit compounds are shown in Table 1. Elemental analyses of three hit compounds can be found in the Supporting Information.

The gene encoding DdlB from *E. coli* JM109 was amplified by PCR using the primers DdlBF 5′-ACTGATAAAATCGCGGTC-CTG-3′ and DdlBR 5′-TTAGTCCGCCAGTTCCAGAATTCG-3′. The resulting product was cloned into pQE-30 UA (Qiagen), sequenced, and transformed into *E. coli* BL21. For overexpression, the resulting strain was grown and lysed as described in the pET manual (Novagen). The enzyme was purified using a nickel affinity resin as described by the manufacturer (Novagen).

Enzyme Inhibition. The D-Ala-adding activity of DdlB ligase was monitored with the colorimetric malachite green method in which orthophosphate generated during the reaction is measured. For the initial screening of compounds obtained from the virtual screening, each compound was tested in duplicate at a concentration of 250 μM for its ability to inhibit DdlB activity. Assays were performed at 37 °C in a mixture (final volume: 50 μL) containing 50 mM Hepes (pH 8.0), 3.25 mM $MgCl_2$, 6.5 mM $(NH_4)_2SO_4$, 700 μM D-Ala, 500 μM ATP, purified DdlB (diluted in 50 mM Hepes (pH 7.2), and 1 mM dithiothreitol), and the test compound. All compounds were soluble in the assay mixture containing 5% DMSO. After 30 min of incubation, 100 μL of Biomol reagent was added, and absorbance was read at 650 nm after 5 min. To exclude possible nonspecific (promiscuous) inhibitors, all compounds were also tested in the presence of Triton X-114 (0.005%).[35] For compounds that showed significant inhibitory activity with respect to a similar assay without the inhibitor, K_i values were determined. K_i determinations were performed under similar conditions using D-Ala (10 mM), ATP (100, 200, 300, and 500 μM), and inhibitor (25, 50, 100, 250, and 500 μM) with 20 min of incubation at 37 °C. Additionally, we performed a study for possible time-dependent inhibition of our three hit compounds. Each

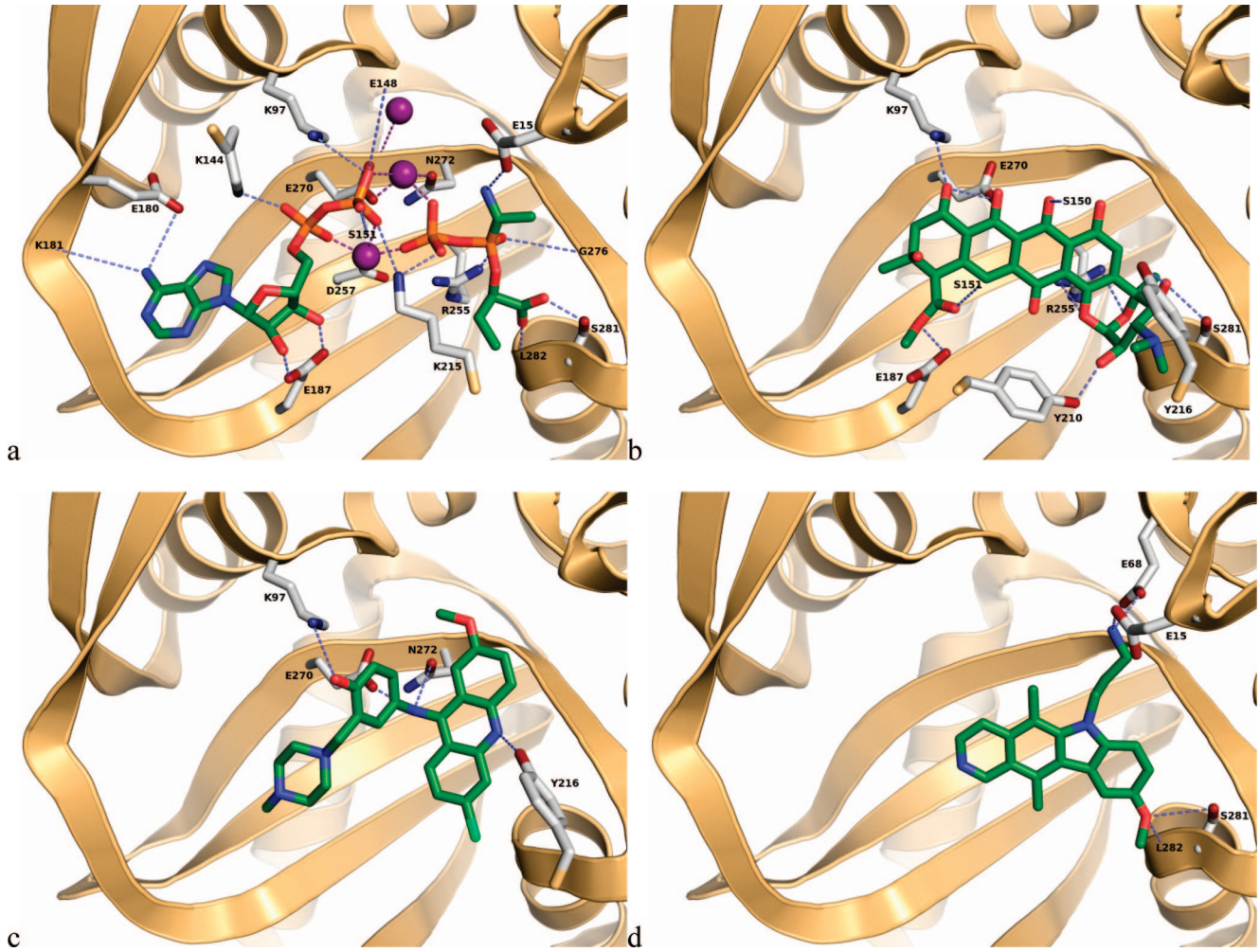

Figure 3. (a) Crystallographic conformation of the DdlB active site including bound substrate, cofactor, and metal ions and low-energy conformations of (b) **8**, (c) **9**, and (d) **10** docked in the DdlB active site. The enzyme is shown with residues 141−157 and 207−217 omitted for clarity. The inhibitors, ADP, POB, and the side chains of interacting residues are represented as sticks and are color coded by element: side chain C, other C, N, O, Cl, and P are gray, green, blue, red, lime green and orange, respectively. Hydrogen bonds are represented as blue dashed lines. Mg^{2+} ions are purple.

compound, at a 250 μM final concentration, was preincubated with the enzyme for 15 min before the reaction was initiated with the addition of substrates (the same final concentrations as those described for the initial screening). After 20 min of incubation at 37 °C, the reaction was terminated in the usual manner with the addition of Biomol reagent. By comparing RA% values in a similar assay with no preincubation, we were able to conclude that inhibitors do not act in a time-dependent manner.

Microbiological Evaluation. Minimal inhibitory concentrations (MICs) of compounds were determined by broth microdilution in IsoSensitest broth (Oxoid) using an inoculum of 10^4 cells per mL for *E. coli* or 10^6 cells per mL for *S. aureus*. The potential antimicrobial agents were prepared in a two-fold dilution series in 50% dimethyl sulfoxide (Sigma-Aldrich). Microwell plates with 96 wells (Nunc, Fisher Scientific), each containing a potential antimicrobial agent and a bacterial suspension, were incubated for 16 h at 37 °C in a Spectramax 384 plus microwell plate reader (Molecular Devices) running the SOFTmax PRO 3.1.1 software. Readings of optical density at 600 nm were made at 10 min intervals. Plates were shaken for 60 s before each reading. The MIC was taken as the lowest concentration of potential antimicrobial agent that prevented the growth of bacteria in a well.

Results and Discussion

Characteristics of the DdlB Active Site. For the docking of the NCI diversity set, we used the crystal structure of D-alanyl-D-alanine ligase from *E. coli* DdlB complexed with an ADP/phosphorylated D-Ala-D-α-hydroxybutyrate phosphonate transition-state inhibitor (POB), as shown in Figure 3a. In this cocrystal structure, several amino acid residues interact with the inhibitor and cofactor. An important electrostatic bond exists between the α-amino group of the N-terminal D-alanine and the carboxylic group of the Glu15 side chain. The terminal COOH group of POB interacts with Ser281 and the backbone amide of Leu282. The oxygen atom of the phosphoryl bond forms two weak hydrogen bonds with the backbone NH group of Gly276 and the amino group of Arg255. The side chain of the C-terminal D-alanine participates in hydrophobic interactions with Tyr210, Lys215, and Tyr216. Three Mg^{2+} ions are present in the crystal structure of the complex, but only two of them are important for bridge formation between ADP and the phosphorylated phosphonate inhibitor. The α- and β-phosphate groups of ADP form electrostatic links with Lys97, Lys144, and Lys215 as well as a hydrogen bond with the backbone NH of Ser151. The adenine ring of ADP binds into the hydrophobic pocket formed by Ile142, Trp182, and Met259, and strong hydrogen bonds further link the ribose ring with Glu187.

Docking Algorithm. AutoDock is used to perform the computational molecular docking of small molecules to proteins by treating the ligand as being conformationally flexible.

AutoDock 4.0 has a free-energy scoring function based on a linear regression analysis of a set of diverse protein−ligand complexes with known inhibition constants. This scoring function uses the AMBER force field to estimate the free energy of binding of a ligand to its target. A hybrid global−local evolutionary algorithm is used to search the phase space of the ligand−macromolecule system.

Control Docking. As a test of the docking algorithm's ability to reproduce the cocrystallized pose of the inhibitor POB, we first docked the inhibitor to the active site of DdlB, from which all ligands have been removed. The docking positions belonging to the lowest energy cluster (the pose was found 11 times out of 100 runs and lowest docked energy was −7.49 kcal/mol) corresponded well to the pose of the cocrystallized inhibitor, with an rmsd of 1.4 Å (Figure 2). The rms deviation of the conformations in the largest cluster (53 similar poses were found in 100 runs) from the cocrystallized inhibitor conformation was 8.2 Å. This was the cluster with the fourth lowest docked energy (−4.38 kcal/mol).

Inhibitors from the National Cancer Institute Diversity Set. In a preliminary docking study of DdlB with Mg^{2+} ions present in the active site, we observed that the steric obstructions imposed by these ions prevent most of the compounds from the NCI diversity set from successfully fitting into the binding cavity. The enzyme's three Mg^{2+} ions are located between the substrate and the ADP binding site and divide the binding cavity into two smaller unconnected cavities, which are unable to accommodate larger compounds. ADP itself also hinders access to the catalytic site, so we elected to remove it and the Mg^{2+} ions from the binding cavity prior to docking. The NCI diversity set was thus docked to the DdlB active site from which all ligands had been removed. Some subsequently identified active compounds docked into the empty enzyme are sterically bulky, for example, compounds **9** (NSC130813) and **10** (NSC176327), and would not dock to the enzyme with either Mg^{2+} or ADP present. Docking results were obtained as a ranked list of structures on the basis of their mean estimated binding free energies. The rank of each compound was determined by the calculated average binding free energy of the most populated cluster. This differs from the ranking strategy employed by other authors, where the estimated free energy of binding of the lowest energy conformation was used to rank compounds. We used this alternative approach because the most populated cluster of conformations more reliably represents an actual pose that a compound may occupy in the binding cavity. Ranking by the lowest docked energy can favor unreliable single-member clusters that are prone to disappear if the docking parameters are modified. The mean energy of the largest cluster is less sensitive to changes in docking parameters, which results in a more stable ranking. Several studies show that in docking calculations the most populated clusters of the docked ligand conformations are better predictors of the native state than the usual approach of selecting the lowest free-energy cluster.[36−39] A study conducted with the participation of the authors of AutoDock showed that the predicted binding energy of the most populated cluster agrees well with the measured binding affinity for a set of ligands.[40]

The 130 top-ranked compounds were selected for an in vitro evaluation of their ability to inhibit DdlB. In 98 of these compounds, the largest cluster coincided with the lowest energy cluster, including our hit compound **8** (NSC86005) that was described in the following section. Compounds **9** and **10** did not follow this rule; their largest clusters were ranked as ninth and third according to their lowest docked energies, respectively. These two compounds were later found to have the best antimicrobial activities.

Three compounds were found to inhibit DdlB with K_i values in the micromolar range. Their structures, K_i values, estimated binding energies, and physicochemical parameters are presented in Table 1. Two of them were ranked as the first two by our ranking strategy. Kinetic analysis reveals that compounds **8** and **10** inhibit the enzyme in ATP-competitive mode with K_i values as low as 42 and 11 μM, respectively, whereas compound **9** is an ATP noncompetitive inhibitor of Ddl with a K_i value of 218 μM. To confirm the potential of these compounds for further development, we evaluated their in vitro antimicrobial activities (Table 1). The MIC of each compound was determined against *E. coli* 1411, *E. coli* SM1411, and *S. aureus* 8325-4. *E. coli* SM1411 is an AcrAB-deficient derivative of *E. coli* 1411 that exhibits increased susceptibility to a range of antimicrobial agents.[41] All three DdlB-inhibitory compounds prevented the growth of *S. aureus* 8325-4. Compounds **9** and **10** accomplished this at concentrations as low as 32 μg/mL. *E. coli* 1411 growth was inhibited by only one compound, **10** with an MIC of 32 μg/mL. Compounds **9** and **10** also prevented growth of *E. coli* SM1411 with MICs of 64 and 8 μg/mL, respectively. An increase in antimicrobial activity against *E. coli* SM1411 compared with that against *E. coli* 1411 indicates that these two compounds may be eliminated from wild-type bacteria through their efflux systems. Very weak antimicrobial activity of compound **8** on *S. aureus* 8325-4 and no antimicrobial activity on *E. coli* strains could be explained by the low permeability (log P = 0.6) and high polar surface area (PSA = 204 Å^2) for this compound (Table 1). Namely, polar surface area should be below 120 Å^2 to allow a molecule to permeate the cell membrane.[42]

Compound **8** is an ATP-competitive inhibitor of DdlB with a K_i value of 42 μM. Structurally, it is a nogalamycin derivative (Table 1) that belongs to the class of anthracycline antibiotics.[43] Anthracycline antibiotics have limited antibacterial use in humans because of their toxicity but have found some applications as antitumor agents.[44] The polar nature of **8**, which is probably detrimental to its performance in microbiological testing, allows the formation of hydrogen bonds with many active site residues, namely, with Lys97, Ser150, Ser151, Glu187, Tyr210, Tyr216, Arg255, Glu270, Ser281, and Leu282. The anthraquinone ring also forms some hydrophobic interactions with the alanine-binding hydrophobic pocket (Figure 3b).

Compound **9** has >90% structural similarity to antimalarial drugs of the aminoalkylphenole type and to the 9-anilinoacridine anticancer agents.[45,46] It has been placed among the best-ranked compounds in several virtual screening tests with anticancer or antiviral targets.[47−49] It is a promising hit compound for further discovery of Ddl inhibitors because it has a K_i of 218 μM and has antimicrobiological activity against both *E. coli* SM1411 and *S. aureus* 8325-4 with MICs of 64 and 32 μg/mL, respectively. The representative docked conformation from the most populated cluster is shown in Figure 3c. The acridine moiety occupies the binding site of both alanines, whereas the piperazine ring is directed into the ATP binding site where it is positioned in the place of ribose, albeit without prominent bonding to Glu187. Tyr216 is predicted to donate a hydrogen bond to the acridine nitrogen atom and Lys97 accepts one from the phenolic OH, whereas Glu270 and Asn272 can both form hydrogen bonds with the exocyclic amino group. The chlorophenyl part of the acridine ring is bound to the D-alanine hydrophobic pocket.

Compound **10** is an analogue of ellipticine, an anticancer agent that acts as an inhibitor of topoisomerase II, DNA chelator, and a multidrug resistance inhibitor.[50] Compound **10** is an ATP-competitive inhibitor of Ddl with a K_i of 11 μM. It showed very promising activity in the microbiological evaluation with MICs against *E. coli* SM1411 and *S. aureus* 8325-4 of 8 and 32 μg/mL, respectively. The representative docked conformation from the most populated cluster is presented in Figure 3d. The docked structure of this molecule is mostly positioned in the substrate binding site. The indole ring of the pyridocarbazole scaffold lies in the alanine-binding hydrophobic pocket. The oxygen of the methoxy group can accept hydrogen bonds from Ser281 and the backbone NH of Leu282. The inhibitor's amino group can donate two H bonds to Glu15 and Glu68.

Conclusions

We have conducted a virtual ligand screening of compounds from the NCI database to identify novel inhibitors of DdlB ligase, an essential enzyme involved in peptidoglycan synthesis. This is the first time AutoDock 4.0 and the NCI diversity set have been used in the discovery of potential antibacterial agents. We tested 130 of the best-ranked compounds and obtained three hits with novel scaffolds. Hit compounds **8** and **10** are ATP-competitive inhibitors with K_i values in the low micromolar range, and compound **9** inhibits the enzyme in a noncompetitive manner. Hits **9** and **10** also possess antibacterial activity and are therefore promising starting points for further optimization.

Acknowledgment. This work was supported by the European Union FP6 Integrated Project EUR-INTAFAR (project no. LSHM-CT-2004-512138) under the thematic priority of Life Sciences, Genomics, and Biotechnology for Health. The support from the Ministry of Higher Education, Science, and Technology of the Republic of Slovenia and the Slovenian Research Agency is also acknowledged. We would like to thank the Drug Synthesis and Chemistry Branch, Developmental Therapeutics Program, Division of Cancer Treatment and Diagnosis, National Cancer Institute for supplying compounds for testing. We thank Dr. G. W. A. Milne for critical reading of the manuscript.

Supporting Information Available: Elemental analyses of hit compounds **8**−**10**. This material is available free of charge via the Internet at http://pubs.acs.org.

References

(1) Labischinski, H.; Maidhof, H. Bacterial Peptidoglycan: Overview and Evolving Concepts. In *Bacterial Cell Wall*; Ghuysen, J.-M., Hakenbeck, R., Eds.; Elsevier: Amsterdam, 1994; pp 23−38.
(2) Barreteau, H.; Kovač, A.; Boniface, A.; Sova, M.; Gobec, S.; Blanot, B. Cytoplasmic steps of peptidoglycan biosynthesis. *FEMS Microbiol. Rev.* **2008**, *32*, 168–207.
(3) Kahan, F. M.; Kahan, J. S.; Cassidy, P. J.; Kropp, H. The mechanism of action of fosfomycin (phosphonomycin). *Ann. N.Y. Acad. Sci.* **1974**, *235*, 364–386.
(4) Neuhaus, F. C.; Lynch, J. L. The enzymatic synthesis of D-alanyl-D-alanine. III. On the inhibition of D-alanyl-D-alanine synthetase by the antibiotic D-cycloserine. *Biochemistry* **1964**, *3*, 471–479.
(5) Walsh, C. T. Enzymes in the D-alanine branch of the bacterial cell wall peptidoglycan assembly. *J. Biol. Chem.* **1989**, *264*, 2393–2396.
(6) Zawadzke, L. E.; Bugg, T. D. H.; Walsh, C. T. Existence of two D-alanine:D-alanine ligases in *Escherichia coli*: cloning and sequencing of the ddlA gene and purification and characterization of the DdlA and DdlB enzymes. *Biochemistry* **1991**, *30*, 1673–1682.
(7) Daub, E.; Zawadzke, L. E.; Botstein, D.; Walsh, C. T. Isolation, cloning, and sequencing of the *Salmonella typhimurium* ddlA gene with purification and characterization of its product, D-alanine:D-alanine ligase (ADP forming). *Biochemistry* **1988**, *27*, 3701–3708.
(8) Healy, V. L.; Mullins, L. S.; Li, X.; Hall, S. E.; Raushel, F. M.; Walsh, C. T. D-Ala-D-X ligases: evaluation of D-alanyl phosphate intermediate by MIX, PIX, and rapid quench studies. *Chem. Biol.* **2000**, *7*, 505–514.
(9) Mullins, L. S.; Zawadzke, L. E.; Walsh, C. T.; Raushel, F. M. Kinetic evidence for the formation of D-alanyl phosphate in the mechanism of D-alanyl-D-alanine ligase. *J. Biol. Chem.* **1990**, *265*, 8993–8998.
(10) Neuhaus, F. C.; Carpenter, C. V.; Miller, J. L.; Lee, N. M.; Gragg, M.; Stickgold, R. A. Enzymatic synthesis of D-alanyl-D-alanine. Control of D-alanine:D-alanine ligase (ADP). *Biochemistry* **1969**, *8*, 5119–5124.
(11) Healy, V. L.; Lessard, I. A; Roper, D. I.; Knox, J. R.; Walsh, C. T. Vancomycin resistance in enterococci: reprogramming of the D-Ala-D-Ala ligases in bacterial peptidoglycan biosynthesis. *Chem. Biol.* **2000**, *7*, R109−R119.
(12) Strominger, J. L.; Ito, E.; Threnn, R. H. Competitive inhibition of enzymatic reactions by oxamycin. *J. Am. Chem. Soc.* **1960**, *82*, 998–999.
(13) Neuhaus, F. C.; Lynch, J. L. The enzymatic synthesis of D-alanyl-D-alanine. III. On the inhibition of D-alanyl-D-alanine synthetase by the antibiotic D-cycloserine. *Biochemistry* **1964**, *3*, 471–480.
(14) Parsons, W. H.; Patchett, A. A.; Bull, H. G.; et al. Phosphinic acid inhibitors of D-alanyl-D-alanine ligase. *J. Med. Chem.* **1988**, *31*, 1772–1778.
(15) Chakravarty, P. K.; Greenlee, W. J.; Parsons, W. H.; Patchett, A. A.; Combs, P.; Roth, A.; Busch, R. D.; Mellin, T. N. (3-Amino-2-oxoalkyl)phosphonic acids and their analogues as novel inhibitors of D-alanine:D-alanine ligase. *J. Med. Chem.* **1989**, *32*, 1886–1890.
(16) Lacoste, A. M.; Chollet-Gravey, A. M.; Vo Quang, L.; Vo Quang, Y.; Le Goffic, F. Time-dependent inhibition of *Streptococcus faecalis* D-alanine:D-alanine ligase by α-aminophosphonamidic acids. *Eur. J. Med. Chem.* **1991**, *26*, 255–260.
(17) Ellsworth, B. A.; Tom, N. J.; Bartlett, P. A. Synthesis and evaluation of inhibitors of bacterial D-alanine:D-alanine ligases. *Chem. Biol.* **1996**, *3*, 37–44.
(18) Duncan, K.; Walsh, C. T. ATP-dependent inactivation and slow binding inhibition of *Salmonella typhimurium* D-alanine:D-alanine ligase (ADP) by (aminoalkyl)phosphinate and aminophosphonate analogues of D-alanine. *Biochemistry* **1988**, *27*, 3709–3714.
(19) McDermott, A. E.; Creuzet, F.; Griffin, R. G.; Zawadzke, L. E.; Ye, Q.-Z.; Walsh, C. T. Rotational resonance determination of the structure of an enzyme-inhibitor complex: phosphorylation of an (aminoalkyl)phosphinate inhibitor of D-alanyl-D-alanine ligase by ATP. *Biochemistry* **1990**, *29*, 5767–5775.
(20) Fan, C.; Moews, P. C.; Walsh, C. T.; Knox, J. R. Vancomycin resistance: structure of D-alanine:D-alanine ligase at 2.3 Å resolution. *Science* **1994**, *266*, 439–443.
(21) Fan, C.; Park, I. S.; Walsh, C. T.; Knox, J. R. D-Alanine:D-alanine ligase: phosphonate and phosphinate intermediates with wild type and the Y216F mutant. *Biochemistry* **1997**, *36*, 2531–2538.
(22) Besong, G. E.; Bostock, J. M.; Stubbings, W.; Chopra, I.; Roper, D. I.; Lloyd, A. J.; Fishwick, C. W.; Johnson, A. P. A de novo designed inhibitor of D-Ala-D-Ala ligase from *E. coli*. *Angew. Chem., Int. Ed.* **2005**, *44*, 6403–6406.
(23) Liu, S.; Chang, J. S.; Herberg, J. T.; Horng, M.-M.; Tomich, P. K.; Lin, A.; Marotti, K. R. Allosteric inhibition of *Staphylococcus aureus* D-alanine:D-alanine ligase revealed by crystallographic studies. *Proc. Natl. Acad. Sci. U.S.A.* **2006**, *103*, 15178–15183.
(24) Kovač, A.; Majce, V.; Lenaršič, R.; Bombek, S.; Bostock, J. M.; Chopra, I.; Polanc, S.; Gobec, S. Diazenedicarboxamides as inhibitors of D-alanine-D-alanine ligase (Ddl). *Bioorg. Med. Chem. Lett.* **2007**, *17*, 2047–2054.
(25) Triola, G.; Wetzel, S.; Ellinger, B.; Koch, M.; Hübel, K.; Rauh, D.; Waldmann H. ATP competitive inhibitors of D-alanine−D-alanine ligase based on protein kinase inhibitor scaffolds. *Bioorg. Med. Chem.* 2008, in press.
(26) Kitchen, D. B.; Decornez, H.; Furr, J. R.; Bajorath, J. Docking and scoring in virtual screening for drug discovery: methods and applications. *Nat. Rev. Drug Discovery* **2004**, *3*, 935–949.
(27) Vernhorst, J.; ter Laak, A. M.; Commandeur, J. N. M.; Funae, Y.; Hiroi, T.; Vermeulen, N. P. E. Homology modeling of rat and human cytochrome P450 2D (CYP2D) isoforms and computational rationalization of experimental ligand-binding specificities. *J. Med. Chem.* **2003**, *46*, 74–86.
(28) Guido, R. V. C.; Oliva, G.; Andricopul, A. D. Virtual screening and its integration with modern drug design technologies. *Curr. Med. Chem.* **2008**, *15*, 37–46.
(29) DeLano, W. L. *The PyMOL Molecular Graphics System*; DeLano Scientific LLC: Palo Alto, CA, 2007.http://www.pymol.org.
(30) The NCI diversity set is available from the Developmental Therapeutics Program, Division of Cancer Treatment and Diagnosis, National Cancer Institute (NCI). The diversity set was selected from a larger repository of compounds at the NCI. See http://dtp.nci.nih.gov/branches/dscb/diversity explanation.html.
(31) Li, C.; Xu, L.; Wolan, D. W.; Wilson, I. A.; Olson, A. J. Virtual screening of human 5-aminoimidazole-4-carboxamide ribonucleotide transformylase against the NCI diversity set by use of autodock to

identify novel nonfolate inhibitors. *J. Med. Chem.* **2004**, *47*, 6681–6690.
(32) Brooks, W. H.; McCloskey, D. E.; Daniel, K. G.; Ealick, S. E.; Secrist, J. A., III; Waud, W. R.; Pegg, A. E.; Guida, W. C. In silico chemical library screening and experimental validation of a novel 9-aminoacridine based lead-inhibitor of human *S*-adenosylmethionine decarboxylase. *J. Chem. Inf. Model.* **2007**, *47*, 1897–1905.
(33) Li, C.; Xu, L.; Wolan, D. W.; Wilson, I. A.; Olson, A. J. Virtual screening of human 5-aminoimidazole-4-carboxamide ribonucleotide transformylase against the NCI diversity set by use of AutoDock to identify novel nonfolate inhibitors. *J. Med. Chem.* **2004**, *47*, 6681–6690.
(34) Rogers, J. P.; Beuscher, A. E.; Flajolet, M.; McAvoy, T.; Nairn, A. C.; Olson, A. J.; Greengard, P. Discovery of protein phosphatase 2C inhibitors by virtual screening. *J. Med. Chem.* **2006**, *49*, 1658–1667.
(35) McGovern, S. L.; Helfand, B. T.; Feng, B.; Shoichet, B. K. A specific mechanism of nonspecific inhibition. *J. Med. Chem.* **2003**, *46*, 4265–4272.
(36) Prasad, J. C.; Goldstone, J. V.; Camacho, C. J.; Vajda, S.; Stegeman, J. J. Ensemble modeling of substrate binding to cytochromes P450: analysis of catalytic differences between CYP_{1A} orthologs. *Biochemistry* **2007**, *46*, 2640–2654.
(37) Källblad, P.; Mancera, R. L.; Todorov, N. P. Assessment of multiple binding modes in ligand−protein docking. *J. Med. Chem.* **2004**, *47*, 3334–3337.
(38) Kozakov, D.; Clodfelter, K. H.; Vajda, S.; Camacho, C. J. Optimal clustering for detecting near-native conformations in protein docking. *J. Med. Chem.* **2005**, *89*, 867–875.
(39) Limongelli, V.; Marinelli, L.; Cosconati, S.; Braun, H. A.; Schmidt, B.; Novellino, E. Ensemble-docking approach on BACE-1: pharmacophore perception and guidelines for drug design. *Chem. Med. Chem.* **2007**, *2*, 667–678.
(40) Rosenfeld, R. J.; Goodsell, D. S.; Musah, R. A.; Morris, G. M.; Goodin, D. B.; Olson, A. J. Automated docking of ligands to an artificial active site: augmenting crystallographic analysis with computer modeling. *J. Comput.−Aided Mol. Des.* **2003**, *17*, 525–536.
(41) O'Neill, A. J.; Bostock, J. M.; Morais Moita, A.; Chopra, I. Antimicrobial activity and mechanisms of resistance to cephalosporin P1, an antibiotic related to fusidic acid. *J. Antimicrob. Chemother.* **2002**, *50*, 839–848.
(42) Kelder, J.; Grootenhuis, P. D. J.; Bayada, D. M.; Delbressine, L. P. C.; Ploemen, J.-P. Polar molecular surface as a dominating determinant for oral absorption and brain penetration of drugs. *Pharm. Res.* **1999**, *16*, 1514–1519.
(43) Hütter, K.; Baader, E.; Frobel, K.; Zeeck, A.; Bauer, K.; Gau, W.; Kurz, J.; Schröder, T.; Wünsche, C.; Karl, W.; Wendisch, D. Viriplanin A, a new anthracycline antibiotic of the nogalamyci group. *J. Antibiot.* **1986**, *9*, 1193–1204.
(44) Bachur, N. R. Anthracycline antibiotic pharmacology and metabolism. *Cancer Treat. Rep.* **1979**, *63*, 817–820.
(45) Burckhalter, J. H.; Tendwick, F. H.; Jones, E. M.; Jones, P. A.; Holcomb, W. F.; Rawlins, A. L. Aminoalkylphenols as antimalarials. II. (Heterocyclic-amino)-α-amino-*o*-cresols; the synthesis of camoquin. *J. Am. Chem. Soc.* **1948**, *70*, 1363–1373.
(46) Denny, W. A. Acridine derivatives as chemotherapeutic agents. *Curr. Med. Chem.* **2002**, *9*, 1655–1665.
(47) Yan, Z.; Sikri, S.; Beveridge, D. L.; Baranger, A. M. Identification of an aminoacridine derivative that binds to RNA tetraloops. *J. Med. Chem.* **2007**, *50*, 4096–4104.
(48) Dorsjuren, D.; Burnette, A.; Gray, G. N.; Chen, X.; Zhu, W.; Roberts, P. E.; Currens, M. J.; Shoemaker, R. H.; Ricciardi, R. P.; Sei, S. Chemical library screen for novel inhibitors of Kaposi's sarcoma-associated herpesvirus processive DNA synthesis. *Antiviral Res.* **2006**, *69*, 9–23.
(49) Bond, A.; Reichert, Z.; Stivers, J. T. Novel and specific inhibitors of a poxvirus type I topoisomerase. *Mol. Pharmacol.* **2006**, *69*, 547–557.
(50) Hägg, M.; Berndtsson, M.; Mandic, A.; Zhou, R.; Shoshan, M. C.; Linder, S. Induction of endoplasmic reticulum stress by ellipticine plant alkaloids. *Mol. Cancer Ther.* **2004**, *3*, 489–497.
(51) Virtual Computational Chemistry Laboratory (VCCLAB), http://www.vcclab.org, 2005.
(52) Molinspiration Property Calculation Service, http://www.molinspiration.com, 2002.

JM800726B